Brain Stimulation 17 (2024) 1045–1047

Contents lists available at ScienceDirect

Brain Stimulation

journal homepage: www.journals.elsevier.com/brain-stimulation

# Quantification of subject motion during TMS via pulsewise coil displacement

*Dear Editor,*

Transcranial Magnetic Stimulation (TMS) has emerged as a significant non-invasive brain stimulation technique for clinical and research applications. Recently, the field has witnessed a remarkable increase in methodological rigor (e.g. Ref. [1]) to address the high intra- and interindividual variance [2] that is often seen for TMS. Despite this commitment towards more reliable and reproducible results, a notable gap persists: the absence of a simple metric to assess and report the stimulation accuracy in terms of coil placement throughout a TMS session. During TMS, coil displacements due to subject or experimenter movements can significantly affect the stimulation of target [3] and off-target regions and thus impede therapeutic or scientific outcomes [4]. Although TMS neuronavigation systems are being used extensively, allowing for precise recordings of *coil placements* and thus *displacements*, no straightforward metric currently exists to quantify this critical factor. In contrast, only computationally complex simulations allow for post-experimental quantification of the induced electric fields (e-fields) in a high-resolution (*voxel-wise-like*) manner [5].

Here, we introduce a metric to quantify the placement accuracy of a TMS coil over the course of a stimulation protocol: pulsewise coil displacement (PCD). PCD quantifies the pulse-to-pulse displacement of the TMS coil, combining three positional (x, y, z) and three rotational parameters (roll, pitch, yaw) in one compound metric, following a rationale similar to framewise displacement (FD [6]) for fMRI. By quantifying the coil displacement with a single metric, PCD provides a meaningful assessment for trial-to-trial stimulation accuracy as well as the overall quality of a TMS session. Due to the focus on coil displacements in contrast to, for example, simulations of the induced e-field, PCD yields the same output, both when used with an individual scan or with a template scan for neuronavigation.

PCD is calculated from tracking data that can be recorded effortlessly with any neuronavigation software, offering granularity at the level of individual pulses, bursts, or stimulation trains. Positional (in mm) and rotational (in °) displacements with respect to a user-selected reference can be calculated for each recorded coil placement. We provide functions within the pyNIBS Python package for importing neuronavigation tracking data from all major neuronavigation systems (e.g., `pynibs.read_triggermarker_localite()` to import displacements, `pynibs.calc_tms_motion_params()` to transform tracking data to coil origin, and `pynibs.compute_pcd()` to compute PCD and its intermediate metrics $PCD_{pos}$ and $PCD_{rot}$). The pyNIBS package can be easily installed via the Python package manager, and since PCD computation involves only simple geometric calculations (see below), only minimal computational resources are required. See gitlab.gwdg.de/tms-localization/papers/pcd for example scripts to import neuronavigation data.

*PCD computation.* First, the positional parameters are transformed from subject space ($X_s$, $Y_s$, $Z_s$) to a TMS-coil-based origin ($X_c$, $Y_c$, $Z_c$; Fig. 1a), allowing for distinct quantification of tangential versus orthogonal (z-direction) coil movements, which yield a linear change of the coil-cortex distance. Second, displacements are calculated for each pulse *n* towards a user-defined reference coil placement. This reference placement can for example be a pre-experimentally defined or optimized coil placement or a functionally defined placement throughout the TMS session. Here, we utilize an optimal coil placement as the reference. Third, positional and rotational parameters are processed independently to yield $PCD_{pos}$ and $PCD_{rot}$: The impact of rotational displacements depends on the coil geometry, as, for example round coils show no differences in cortical stimulation for different yaw angles (Fig. 1a), while figure-of-eight coils yield different e-field patterns outside the stimulation cone. Similarly, effects of rotational displacements will differ across pulse shapes, TMS intensities [7], functional domains, and cortical regions [8].

To enable the quantification of coil displacements independent of a specific coil model and other TMS parameters, pitch and roll deviations of the *coil* are transformed into positional displacements on the *cortex* for a given skin-cortex distance (SCD), here assumed to be 20 mm as this is a typical minimal cortical depth for TMS targets (see SI for details on this projection). Users can adjust the SCD parameter by changing the `skin_cortex_distance` parameter of `pynibs.compute_pcd()`, although we recommend using the default value to allow for comparison across sessions and studies. Yaw deviations, i.e., tangential rotations (Fig. 1), are included as $sin(yaw)$ and scaled with SCD to weigh all three rotational parameters in a similar manner.

$Z_c$ displacements from an optimal coil placement yield quadratic changes in the target stimulation due to the orthogonal definition of $Z_c$ towards the skin surface. As differences in contact pressure can lead to (small) displacements towards the head, we also encode the direction of $\Delta z_c$ via $sign(\Delta z_c)$, although the majority of $Z_c$ displacements are expected to happen in positive direction, i.e., away from the head. In contrast, $X_c$ and $Y_c$ displacements from the optimal placement reduce the target stimulation in a manner described by the Euclidean distance, calculated as $\sqrt{\Delta x_c^2 + \Delta y_c^2}$ due to the tangential definition of $X_c$ and $Y_c$ towards the skin surface. Finally, for each pulse *n*, PCD is defined as the sum of positional and rotational displacements:

$$PCD_{pos\_n} = \sqrt{\Delta x_{cn}^2 + \Delta y_{cn}^2} + \Delta z_{cn}^2 \cdot sign(\Delta z_{cn})$$

$$PCD_{rot\_n} = SCD \cdot sin(\Delta yaw_n) + cortex\_projection(\Delta pitch, \Delta roll, SCD)$$

$$PCD_n = PCD_{pos\_n} + PCD_{rot\_n}$$

*PCD validation via e-fields.* We created a large set of virtual TMS experiments with realistic coil drifts to sample pulse-to-pulse coil

https://doi.org/10.1016/j.brs.2024.08.009
Received 14 May 2024; Received in revised form 27 August 2024; Accepted 27 August 2024
Available online 28 August 2024

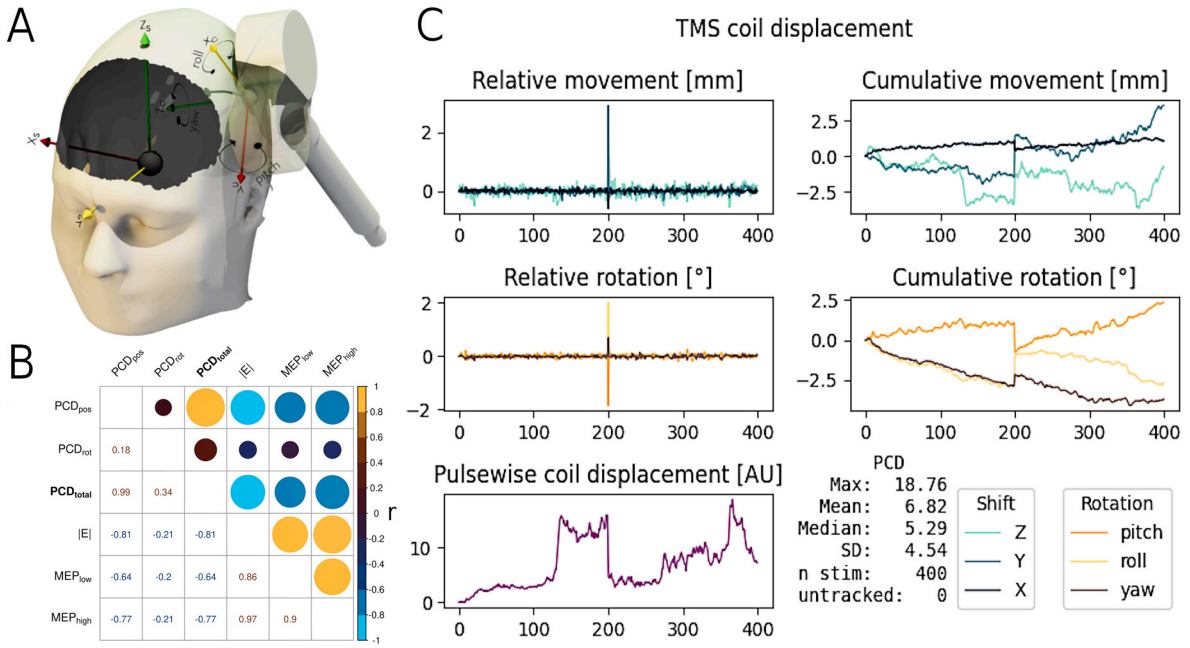


**Fig. 1. Pulsewise coil displacement (PCD) combines positional and rotational displacements of the TMS coil in one metric.** A) The TMS coil is tracked via neuronavigation in the individual subject-space ($X_s$, $Y_s$, $Z_s$), with the origin within the brain. The orientation of the coil (yaw, pitch, roll) is tracked based on a coil-centered coordinate system ($X_cY_cZ_c$). To calculate PCD, the positional coil displacements, i.e., shifts in ($X_s$, $Y_s$, $Z_s$) direction, are transformed into ($X_c$, $Y_c$, $Z_c$) shifts to allow meaningful interpretation, such as shifts in z-direction quantifying changes of the coil-cortex-distance. B) PCD correlates with the induced electric field at the stimulation target. Coil position ($PCD_{pos}$) and coil rotation ($PCD_{rot}$) displacements affect cortical stimulation exposure, quantified as the overall stimulation strength |E|. PCD yields high correlation strength ($r = -0.81$) with |E| at the stimulation target and slightly lower for correlations with simulated MEPs at motor threshold ($MEP_{low}$) and at the upper saturation range ($MEP_{high}$). Data based on 100 simulated random walks of 501 pulses each, yielding 50,100 simulations. C) Output from `pynibs.compute_pcd()`. Experimental data were obtained from a double, spaced $cTBS_{600}$ study with a break after 200 bursts. X-axes: Burst number. Cumulative displacements are presented for visual inspection only. PCD integrates displacement information from all six displacement variables and provides time-series data and summary statistics.

displacements. Starting with an optimal coil placement for a cortical target [9], we computed 500 subsequent coil placements in a random walk fashion, including positional and rotational displacements concurrently. This was repeated 100 times, yielding 50,100 coil positions/orientations across 100 virtual experiments. For each coil placement, the e-field was calculated with SimNIBS (v4.5 beta; [10,11]) to validate the PCD metric with respect to changes in local stimulation exposure. Please refer to the SI for details on the random coil walk and e-field simulation. We extracted the grey matter e-field magnitude at the predefined target ($|E|_{target}$) in a 1 mm grey-matter-only sphere. Both compound metrics, $PCD_{pos}$ and $PCD_{rot}$, were significantly correlated with $|E|_{target}$ ($r(PCD_{pos}, |E|_{target}) = -0.81$; $r(PCD_{rot}, |E|_{target}) = -0.21$; both $p < 0.001$). PCD, the sum of $PCD_{pos}$ and $PCD_{rot}$, yielded a correlation of similar height with $|E|_{target}$ ($r(PCD, |E|_{target}) = -0.81$) (Fig. 1b). Compared to Euclidean error quantifications, which sum the magnitude of displacements, $PCD_{total}$ outperforms these approaches significantly (see SI for details). As expected, Euclidean error metrics are highly correlated with PCD submetrics and it should be noted that these alternative quantification approaches might provide an alternative strategy to quantify coil displacement. As coil displacements not only yield stimulation changes at the cortical target, but also at off-target regions, we also extracted the e-field at two anatomically plausible off-targets at the same cortical depth (see SI for details). Depending on the off-target location, either $\Delta x_c$ or $\Delta y_c$ yield increases of |E|. Compared to the real target, $\Delta z_c$ shows decreased relevance for |E|. $r(PCD, |E|_{off-target})$ is higher than any sub-metric with |E| at these off-target regions (Fig. S3).

*PCD validation via simulated MEPs.* Based on the realized e-fields at the cortical target, we computed motor evoked potentials (MEPs) based on the dual variability source model (DVS; [12]; see SI for details on the implementation). By upscaling the e-fields, we generated two kinds of MEPs: $MEP_{low}$ at the motor threshold and $MEP_{high}$ at the saturation range of the input-output curve. With this analysis, we showcase the relationship between PCD and displacement-dependent changes of a corticospinal response as a proxy of displacement-dependent changes of cortical modulation per se. Utilizing the DVS approach does not take the directional sensitivities of neuronal activation into account [7], thus most probably underestimating the effect of $PCD_{rot}$. As expected, PCD shows slightly lower, albeit still strong correlation with the two MEP types relative to |E|: $r(PCD, MEP_{low}) = -0.62$; $r(PCD, MEP_{high}) = -0.77$ (Fig. S2).

*Real world data.* We include a PCD computation for a recently completed cTBS study in our lab [13]. This study combined a double, spaced $cTBS_{600}$ protocol (i.e., two $cTBS_{600}$ trains over the same area with a break of 10 minutes [14]) with manual coil handling for a right-hemispheric target (Fig. 1c). PCD distills information from all six displacement sources, including the renewed placement at the beginning of the second $cTBS_{600}$ train and the compensation placements at the end of the sessions when head motion increased. In addition to time-series PCD values, summary statistics across the session are provided.

In summary, PCD combines positional and rotational displacements in a single value per TMS pulse, burst, or train, allowing an easy and direct assessment of coil displacements. Comparing PCD to displacement-dependent changes of the cortical stimulation exposure, we show that PCD parallels these changes at the cortical target to a high degree and, to a lesser degree, for cortical off-targets. Besides cortical stimulation exposure, PCD also reflects changes in cortical responses due to coil displacements as shown via simulated MEPs. Thus, we believe that PCD captures relevant information across functional domains, outcome metrics and stimulation paradigms, which should be demonstrated in future studies. Importantly, PCD requires neither individual

structural MRI scans nor complex e-field simulations nor the definition of cortical targets versus off-targets – a task involving a cascade of critical decisions [15] –, as PCD is computed solely on the coil placements, which are readily available from any neuronavigation system. We hope this example of utilizing coil displacement data will encourage researchers to track, record, analyze, and share these valuable data. Besides use-cases including *quality control, intervention monitoring*, and as a *trial-wise exclusion criterion*, PCD might also be used as an *explanatory variable* in higher-level statistical models to help identify stimulation effects.

## CRediT authorship contribution statement

**Ole Numssen:** Writing – review & editing, Writing – original draft, Visualization, Validation, Software, Methodology, Investigation, Formal analysis, Data curation, Conceptualization. **Sandra Martin:** Writing – review & editing, Writing – original draft, Visualization, Validation, Software, Methodology, Investigation, Formal analysis, Conceptualization. **Kathleen Williams:** Writing – review & editing, Writing – original draft, Investigation, Formal analysis, Data curation, Conceptualization. **Thomas R. Knösche:** Writing – review & editing, Writing – original draft, Supervision, Resources, Project administration, Methodology, Funding acquisition, Formal analysis. **Gesa Hartwigsen:** Writing – review & editing, Writing – original draft, Supervision, Resources, Project administration, Funding acquisition.

## Declaration of competing interest

The authors declare that they have no known competing financial interests or personal relationships that could have appeared to influence the work reported in this paper.

## Acknowledgements

G.H. was supported by the European Research Council (ERC) (ERC-2021-COG 101043747), the German Funding Agency (Deutsche Forschungsgemeinschaft; DFG) (HA 6314/4-2 and HA 6314/10-1), and Lise Meitner Excellence Funding by the Max Planck Society. O.N. was supported by grant 01GQ2201 of the Federal Ministry of Education Germany (Bundesministerium für Bildung und Forschung, BMBF), awarded to T.R.K.

## Appendix A. Supplementary data

Supplementary data to this article can be found online at https://doi.org/10.1016/j.brs.2024.08.009.

## References

[1] Caulfield KA, Fleischmann HH, Cox CE, Wolf JP, George MS, McTeague LM. Neuronavigation maximizes accuracy and precision in TMS positioning: evidence from 11,230 distance, angle, and electric field modeling measurements. Brain Stimul 2022;15(5):1192–205. https://doi.org/10.1016/j.brs.2022.08.013.

[2] Siddiqi SH, Kording KP, Parvizi J, Fox MD. Causal mapping of human brain function. Nat Rev Neurosci 2022;23(6):361–75. https://doi.org/10.1038/s41583-022-00583-8.

[3] Koehler M, Kammer T, Goetz S. How coil misalignment and mispositioning in transcranial magnetic stimulation affect the stimulation strength at the target. Clin Neurophysiol 2024;162:159–61. https://doi.org/10.1016/j.clinph.2024.03.037.

[4] Grosshagauer S, Woletz M, Vasileiadi M, Tik M, Linhardt D, Windischberger C. Motion tracking for real-time measurements of coil-cortex distance: a novel approach for improving dose consistency in concurrent TMS/fMRI. Brain Stimul: Basic, Translational, and Clinical Research in Neuromodulation 2023;16(1):323. DOI: 10.1016/j.brs.2023.01.600.

[5] Numssen O, Zier AL, Thielscher A, Hartwigsen G, Knösche TR, Weise K. Efficient high-resolution TMS mapping of the human motor cortex by nonlinear regression. Neuroimage 2021;245:118654. https://doi.org/10.1016/j.neuroimage.2021.118654.

[6] Power JD, Mitra A, Laumann TO, Snyder AZ, Schlaggar BL, Petersen SE. Methods to detect, characterize, and remove motion artifact in resting state fMRI. Neuroimage 2014;84:320–41. https://doi.org/10.1016/j.neuroimage.2013.08.048.

[7] Souza VH, Nieminen JO, Tugin S, Koponen LM, Baffa O, Ilmoniemi RJ. TMS with fast and accurate electronic control: measuring the orientation sensitivity of corticomotor pathways. Brain Stimul 2022;15(2):306–15. https://doi.org/10.1016/j.brs.2022.01.009.

[8] Numssen O, van der Burght CL, Hartwigsen G. Revisiting the focality of non-invasive brain stimulation–Implications for studies of human cognition. Neurosci Biobehav Rev 2023;149:105154. https://doi.org/10.1016/j.neubiorev.2023.105154.

[9] Weise K, Numssen O, Kalloch B, Zier AL, Thielscher A, Haueisen J, Hartwigsen G, Knösche TR. Precise motor mapping with transcranial magnetic stimulation. Nat Protoc 2022;18(2):293–318. https://doi.org/10.1038/s41596-022-00776-6.

[10] Puonti O, Van Leemput K, Saturnino GB, Siebner HR, Madsen KH, Thielscher A. Accurate and robust whole-head segmentation from magnetic resonance images for individualized head modeling. Neuroimage 2020;219:117044. DOI: 10.1016/j.neuroimage.2020.117044.

[11] Thielscher A, Antunes A, Saturnino GB. Field modeling for transcranial magnetic stimulation: a useful tool to understand the physiological effects of TMS?. In: 37th annual international conference of the IEEE engineering in medicine and biology society (EMBC). Milan, Italy; 2015. p. 222–5. https://doi.org/10.1109/embc.2015.7318340.

[12] Goetz SM, Luber B, Lisanby SH, Peterchev AV. A novel model incorporating two variability sources for describing motor evoked potentials. Brain stimulation 2014;7(4):541–52.

[13] Williams K, Numssen O, Bzdok D, Hartwigsen G. Stimulation-induced inhibition of the inferior parietal lobe triggers adaptive network interactions. Organization for Human Brain Mapping (OHBM) conference, Montréal 2023. Canada.

[14] Goldsworthy MR, Pitcher JB, Ridding MC. Neuroplastic modulation of inhibitory motor cortical networks by spaced theta burst stimulation protocols. Brain Stimul 2013;6(3):340–5. https://doi.org/10.1016/j.brs.2012.06.005.

[15] Van Hoornweder S, Nuyts M, Frieske J, Verstraelen S, Meesen RL, Caulfield KA. Outcome measures for electric field modeling in tES and TMS: a systematic review and large-scale modeling study. Neuroimage 2023:120379. DOI: 10.1016/j.neuroimage.2023.120379.

Ole Numssen*
*Methods and Development Group Brain Networks, Max Planck Institute for Human Cognitive and Brain Sciences, Leipzig, Germany*
*Research Group Cognition and Plasticity, Max Planck Institute for Human Cognitive and Brain Sciences, Leipzig, Germany*

Sandra Martin, Kathleen Williams
*Research Group Cognition and Plasticity, Max Planck Institute for Human Cognitive and Brain Sciences, Leipzig, Germany*

Thomas R. Knösche[1]
*Methods and Development Group Brain Networks, Max Planck Institute for Human Cognitive and Brain Sciences, Leipzig, Germany*
*Technische Universität Ilmenau, Institute of Biomedical Engineering and Informatics, Ilmenau, Germany*

Gesa Hartwigsen[1]
*Research Group Cognition and Plasticity, Max Planck Institute for Human Cognitive and Brain Sciences, Leipzig, Germany*
*Wilhelm Wundt Institute for Psychology, Leipzig University, Germany*

* Corresponding author.
*E-mail address:* numssen@cbs.mpg.de (O. Numssen).

[1] shared contribution.